CORTEX 149 (2022) 226–245

Available online at www.sciencedirect.com

ScienceDirect

Journal homepage: www.elsevier.com/locate/cortex

Registered Report

Endogenous modulation of delta phase by expectation—A replication of Stefanics et al., 2010

Sophie K. Herbst [a,*], Gabor Stefanics [b] and Jonas Obleser [c,d]

[a] Cognitive Neuroimaging Unit, NeuroSpin, INSERM, CEA, CNRS, Université Paris-Saclay, France
[b] Translational Neuromodeling Unit (TNU), Institute for Biomedical Engineering, University of Zurich & ETH Zurich, Switzerland
[c] Department of Psychology, University of Lübeck, Lübeck, Germany
[d] Center of Brain, Behavior, and Metabolism, University of Lübeck, Lübeck, Germany

ARTICLE INFO

Article history:
Protocol received 20 November 2019
Protocol accepted 17 June 2020
Received 25 November 2021
Reviewed 23 December 2021
Revised 31 January 2022
Accepted 1 February 2022
Action editor Chris Chambers
Published online 11 February 2022

Keywords:
Expectation
Reaction time
Task relevance
Delta oscillations
EEG
Phase consistency

ABSTRACT

The human brain efficiently extracts the temporal statistics of sensory environments and automatically generates expectations about future events. An influential Hypothesis holds that these expectations can find their implementation in neural oscillations, notably in the delta band (.5–3 Hz). Rhythmic fluctuations of cortical excitement are thought to align and match up in phase to the temporal structure of the sensory environment. This alignment is thought to result in the more excitable phase range of neural oscillations to overlap with the predicted onset of sensory events which in turn results in more efficient processing of sensory input, especially so in audition. An unresolved issue concerns whether such phase-aligned rhythmic brain activity is driven exclusively by the exogenous temporal structure of the input, or whether it also reflects phase re-alignment due to endogenous expectations based on stimulus probability and task relevance. In a seminal study, Stefanics et al. (2010) presented stimuli in a rhythmic stream and observed that delta phase consistency across trials was modulated by endogenous target onset expectations: delta phase consistency was higher prior to more probable (strongly expected) compared to less probable (weakly expected) target onsets. The present study replicates Experiment II of the original study, most importantly the modulation of delta phase consistency by endogenous expectations, and underlines a direct relationship between phase locking and behaviour. Our additional analyses locate the sources of the delta phase-alignment to motor, premotor, parietal, and temporal areas, and provide evidence for an ongoing delta oscillation, in line with the interpretation of oscillatory phase alignment rather than a transient evoked response. Importantly, this work shows that the phase of delta oscillations can be modulated by top-down control, and hence qualifies as a potential mechanism for the neural implementation of (rhythmic) temporal predictions.

* *Corresponding author*. Cognitive Neuroimaging Unit, NeuroSpin, INSERM, CEA, CNRS, Université Paris-Saclay, Bât 145, Gif s/ Yvette 91190, France.
E-mail address: ksherbst@gmail.com (S.K. Herbst).
https://doi.org/10.1016/j.cortex.2022.02.001

1. Introduction

Natural sensory environments commonly feature rhythmic or quasi-periodic temporal structures. In particular, auditory inputs are constrained by rhythms at slow frequencies (Arnal & Giraud, 2012; Ding et al., 2017; Giraud & Poeppel, 2012; Jones & Boltz, 1989), which can facilitate the perceptual analysis of complex dynamic inputs. A large body of research has shown that rhythmic input structures improve the detectability and processing speed of auditory stimuli (Henry & Obleser, 2012; Herrmann et al., 2016; Lawrance et al., 2014; Rimmele et al., 2010; Stefanics et al., 2010; Wright & Fitzgerald, 2004), as well as perceptual sensitivity (Chang et al., 2019; Jones et al., 2002; Morillon et al., 2016; Schmidt-Kassow et al., 2009; but see; Bauer et al., 2015).

Endogenously rhythmic brain dynamics prominently observed across species (Buzsáki & Draguhn, 2004), have been hypothesized to provide an internal temporal structure on which external rhythms can be mapped (Herrmann & Henry, 2014; Jones, 1976; Jones et al., 2002; Large & Jones, 1999). An influential proposal holds that slow neural oscillations, notably in the delta frequency band (.5–3 Hz), coordinate inter- and cross-modal attentional selection in time by aligning in phase to an external rhythmic structure (Lakatos et al., 2008; Schroeder & Lakatos, 2009), allowing to match states of high excitability with the expected onsets of future sensory events. Accordingly, a host of studies using electrophysiological recordings of neural oscillations in humans have revealed evidence for phase alignment to rhythmic inputs leading to modulation of behavior (Arnal et al., 2015; Besle et al., 2011; Cravo et al., 2013; Henry et al., 2014; Henry & Obleser, 2012; Kösem et al., 2014; Morillon & Baillet, 2017; Stefanics et al., 2010; van den Brink et al., 2014). In the literature, a number of terms exist to describe the phenomenon of synchronization between internal and external rhythms (Lakatos et al., 2019; Obleser & Kayser, 2019), such as *phase locking*, *phase consistency*, *entrainment*, and more. Here, we are interested in the *alignment* of the phase of neural oscillations to an external rhythm, which surfaces as *phase consistency across trials*.

The overlap between external and internal rhythms raises the question to which extent the observed phase consistency across trials reflects *entrainment* of an endogenous oscillation (Lakatos et al., 2019; Obleser & Kayser, 2019), versus a mechanistically driven representation of the exogenous periodicity. An active role of entrainment in the attentional selection process is suggested by its susceptibility to top-down influences such as the attended sensory modality (Keil et al., 2016; Lakatos et al., 2008), task demands (Lakatos et al., 2013), perceptual grouping (Barczak et al., 2018), and hierarchical rhythmic structure (Morillon & Baillet, 2017; Nozaradan et al., 2011). A seminal study by Stefanics et al. (2010) showed that phase consistency of delta oscillations in the presence of an exogenous rhythm scales with the strength of the expectation for a behaviorally relevant stimulus to occur in the next cycle of a rhythmic stimulus stream. This result suggests that oscillatory phase alignment can be modulated endogenously to create a temporally transient state of expectation.

A different set of studies have tested whether delta oscillations implement endogenous temporal predictions, independently from periodic input structures. These studies used foreperiod paradigms (Niemi & Näätänen, 1981; Woodrow, 1914) in which temporal predictions are conveyed by single time intervals and need to be initiated on each trial (Breska & Deouell, 2017; Cravo et al., 2011; Herbst & Obleser, 2017, 2018; Wilsch et al., 2015).

Only very few studies reported enhanced delta phase consistency in a non-rhythmic context (Breska & Deouell, 2017, Daume et al., 2021; but see Obleser et al., 2017) and for temporal predictions evoked by the passage of time (Wilsch et al., 2015) using auditory stimuli, and one study reported enhanced phase consistency for temporally predicted visual stimuli in theta band (4–7 Hz, Cravo et al., 2011). In three independent EEG experiments (total N = 70), using non-rhythmic foreperiod manipulations, we did not observe phase consistency effects in the delta band *prior* to an expected target onset (Herbst & Obleser, 2017, 2018). However, we have been able to show that listeners can flexibly form temporal predictions associated to sensory features of temporal cues on a trial-by-trial basis (Herbst & Obleser, 2019), and that these predictions enhance auditory sensitivity. Furthermore, using encoding-models, we could show that temporal predictions are represented in human brain dynamics measured with EEG (Herbst et al., 2018). In Herbst and Obleser (2019) we report a relationship between the phase of delta oscillations and auditory sensitivity in a temporally predictive condition, which suggests a role of delta oscillations for non-rhythmic temporal predictions.

Thus, to date, it remains an open question to which extent the phase of cortical delta oscillations encodes *endogenous* expectations derived from exogenous temporal structures. As the basis for an extended research program aiming at a better understanding of the conditions under which delta oscillations could implement endogenous expectations, we here set out to replicate the study described under Experiment II by Stefanics et al. (2010). This study consists in an important basis for the research field outlined above, and at the time the current study was planned, the paper was cited 297 times. Human participants responded to pure tone stimuli, embedded in a rhythmic stream in which pitch cues indicated whether a target occurred in the following first or second cycle with 20/80% versus 80/20% probability. The authors reported a decrease in reaction times for targets occurring at the expected time points, and, crucially, relatively enhanced phase consistency in the delta band (.5–3 Hz) at time points for which strong (80%) versus weak (20%) expectations existed.

Importantly, a hallmark feature of to-be replicated study, and an important part of our motivation to chose it for replication, was its careful avoidance of confounding stimulus-evoked with pre-stimulus activity (Zoefel & Heil, 2013). By showing a modulation of stimulus-related rhythmic brain dynamics by expectation, the original study, and now the replication, provide important evidence for an endogenous implementation of expectations in oscillatory brain dynamics.

Here, we replicate the increase in delta phase consistency with expectation, which also correlated with the reaction time benefits across individuals. In addition, we also examined whether the measured phase consistency qualifies as an

endogenous narrow-band oscillation that *entrains* to the stimulus rhythm, versus reflects more broad-band neural activity. To achieve this, we performed additional spectral analyses on the data, and also assessed phase consistency effects in the low delta (.25–1.5 Hz) and theta (4–7 Hz) band.

To date, it is an open question to what extent the above-described oscillatory brain dynamics overlap with well-known signatures of expectation observed in the time domain (both pre- and post-stimulus), such as the contingent negative variation (Brunia, 2003; Mento, 2013; Walter et al., 1964), and the P300 (Ruchkin et al., 1980; Schröger et al., 2015; Schürmann et al., 2001), for which the original study reported a partial overlap between with delta phase consistency. In our view, it is possible that these different potentials result at least partially from a phase-reset of delta oscillatory activity (Lakatos et al., 2008; Schürmann et al., 2001), and thus provide separate observation windows onto the same neural activity.

Here, we addressed the overlap between oscillatory and time-domain measures, by performing a set of control analyses in the spectral and temporal domain. Yet, a complete account of their respective nature will require a variety of study designs (varying time windows, modalities, task requirements) and recording techniques (invasive recordings, enhanced spatial resolution such as in MEG).

1.1. *Hypotheses*

In order to consider the replication successful, we assessed two main hypotheses:

Hypothesis 1. We expected to find a facilitatory effect of expectation on reaction times, that is, shorter reaction times for targets that occur at the expected versus non-expected point in time. This effect was supposed to be more pronounced at the short compared to the long time interval **(confirmed)**.

Hypothesis 2. We expected to find that the strength of phase consistency in the delta band scales with the expectation, such that stronger phase consistency would be observed when the expectation for a target to occur was high **(confirmed)**.

Additionally, we assessed several exploratory hypotheses:

Hypothesis 3. We expected to be able to isolate a peak in the EEG power spectrum that corresponds to the stimulation frequency, separable from the 1/f scale-free activity **(confirmed)**.

Hypothesis 4a. We expected the amplitude of target-evoked, broad-band responses to differ between expected and unexpected targets, with no prior hypothesis on the direction for this difference **(post-target difference not confirmed, but pre-target difference observed)**.

Hypothesis 4b. We expected to see an omission response shortly after the time point of the early target onset, but when no target occurred, with a larger amplitude on trials on which expectation was stronger **(not confirmed)**.

Hypothesis 4c. Correlation analyses were expected to show partial, but not full overlap between the time domain signatures of expectation and delta phase consistency **(confirmed)**.

Hypothesis 5. Following the confirmation of Hypothesis 2, we reconstructed the sources of the differences in delta phase consistency, expecting them to lie mainly in auditory and possibly also motor areas **(confirmed)**.

The preregistered Stage 1 report can be found under this link: https://osf.io/w5eq4/.

2. Methods

The auditory stimulation protocol was kept exactly as in the original study (Stefanics et al., 2010). A visual display, which was not mentioned in the original study, was added to guide the participant throughout the task (see below). Due to methodological advances in EEG research since the date of the original study, and the available facilities, our (preregistered: https://osf.io/w5eq4/) analysis approach differed in some aspects from the to-be-replicated study. All deviations from the original analysis approach are thought to reflect advances that should in all likelihood help to uncover true effects and estimate their size more accurately.

2.1. *Participants*

2.1.1. *Ethical approval*

Ethical approval was obtained from the ethics committee of the University of Lübeck. All participants signed informed consent and received either course credit or payment for their participation (10 € per hour).

2.1.2. *Final participant sample*

The 26 participants considered for analysis had an average age of 23.61 years (SD: 3.56), ten were male (ratio: 38.46%), and 21 were right-handed. Participants had no history of neurological or hearing disorder. The original study tested 11 participants (6 female, no mention of handedness).

Using the stopping rule described below, we tested 28 participants, one of which was excluded due to an abortion of the recording program, resulting in only 700 trials (see exclusion criteria below), and one due to too many trials rejected during EEG preprocessing (566 trials left).

2.1.3. *Stopping rule*

Here, we applied an optional stopping approach using Bayes Factors (Rouder, 2014), to assess the two main Hypotheses (the exact statistical tests are described in the Analyses section:

Hypothesis 1. Reaction times are relatively shorter for strong versus weak expectations.

Hypothesis 2. Delta phase consistency is relatively higher for strong versus weak expectations.

Hypothesis 1 was confirmed, reaching a Bayes Factor of 3464.96. Concerning Hypothesis 2, we reached confirmatory Bayes Factors of 7.40 (delta band), and 14.37 (low delta band).

We initially stopped data recording at a Bayes Factor of 17 in favour of Hypothesis 2 (delta band), which turned out inflated due to a coding error and now lies at 7.40. Since the results converge well across the different analyses, with the cluster-based permutation tests revealing robust levels of significance, we decided to not take up testing again. The number of 26 participants included already more than doubles that of the original study (N = 11).

2.1.4. Recruitment criteria

Initially, we invited 15 participants, and then continued until reaching conclusive Bayes Factors for both Hypotheses 1 & 2: either >10 in favour of the respective Hypothesis, or <0.1 in favour of the corresponding H_0. Due to practical constraints in recruiting and testing participants, we invited participants in groups of five, and assessed the Bayes Factors after each group until we reached the target Bayes Factor. The final number of 28 participants tested (not a multiple of five) resulted from cancellations by participants. Left- and right-handed participants were recruited with a gender imbalance no larger than 60:40. Participants were required to have no history of neurological or hearing disorder. If upon testing 50 participants we would not have reached a conclusion on both hypotheses, we would have stopped the data collection, reported the results as inconclusive, and considered the replication attempt as failed. Exclusion criteria are listed below.

2.1.5. Recording abortion criteria

Participants were granted the right to stop the experiment at any time without specifying a reason. Furthermore, the experimenter could terminate the recording session in case of technical problems that either made a recording impossible or would have led to insufficient data quality.

2.1.6. Post-recording participant exclusion criteria

Participants whose average reaction time exceeded 500 msec would have been excluded from the study (applied to zero participants). This criterion was based on the data shown in Fig. 1 in the original study, from which we calculated that the mean reaction time for the slowest condition plus three times its standard deviation resulted in 375 msec. Furthermore, we excluded participants for whom we obtained less than 75% of useable EEG trials per condition of interest (300 and 75 trials, respectively), either due to early abortion of testing, or due to a high number of trials rejected during the EEG data preprocessing (applied to two participants).

2.1.7. Timeline

Following the acceptance of first-stage preregistration, we immediately proceeded to testing participants. The data collection and preregistered analyses were concluded within one and a half years.

2.1.8. Data and code availability

Due to less stringent standards for data storage at the time the original study was recorded, these data are no longer available, which further motivated the replication attempt. Anonymized behavioral, as well as the raw and preprocessed EEG data are available on the Open Science Framework, together with the analysis code written in Matlab and R: https://osf.io/u24tn/.

2.2. Experimental paradigm

The experimental paradigm was implemented using the Psychophysics Toolbox (Brainard, 1997; Pelli, 1997) under Windows 7, using a Black Box Toolkit USB response pad for response collection. Participants were instructed to use the index finger of the right hand to respond. The EEG recordings took place in an electrically shielded sound-attenuated EEG booth at the Center of Brain, Behavior and Metabolism (CBBM) at the University of Lübeck, Germany.

Participants were presented with cue-target pairs of pure tone auditory stimuli, embedded in a rhythmic stream (depicted in Fig. 1), and instructed to perform a speeded response to the target. Cues and targets were separated by an interval of 1350 msec or 2700 msec, with an inter-trial interval of 1350 msec, such that stimulation was fully periodic at a frequency of .74 Hz. Tones were presented via headphones at 70 dB SPL, the cue tones at 1046 and 1318 Hz, and the targets at 1975 Hz. Cue tones had a duration of 150 msec, and targets a duration of 50 msec, both with 10 msec rise and fall times. Crucially, the cue tone's frequency was probabilistically associated with the temporal onset of the target tone, indicating whether the target is more likely to occur at the first (1350 msec), or second possible time point (2700 msec) with a 20% versus 80% or 80% versus 20% probability-ratio. Short and long cue-target intervals (SOAs), and accordingly the cues associated with them, were balanced with a 50/50% ratio, and presented in random order. While the original study mentions no reversal of the assignment between cue frequency and target onset time over participants, we here switched the assignment for every second participant. The relevance and meaning of the cues was fully disclosed to participants prior to the experiment.

Throughout the whole experiment, participants were asked to fixate a black fixation cross on a gray background. Written instructions were presented on the screen, including the information about the temporal contingencies between cue and target tones. If a participant pressed the response-button before the target, a red 'x' was presented for .2 sec. Otherwise, directly after the response, the fixation cross turned white for .2 sec to indicate that a response was registered. If no response was given, a black 'x' was displayed for .2 sec.

After a short training on the task (50 trials, average trial duration of 3375 msec), participants performed 1000 trials (500 per cue type) divided into 10 blocks. After each block, the number of missed and early trials (response prior to target onset) were written on the screen, and participants took a break of minimally 60 sec and continued the experiment after a self-determined time. For the EEG analyses, this resulted in 100/400 trials at which unexpectedly/expectedly no target occurred at the early time point (minus outlier trials, see below).

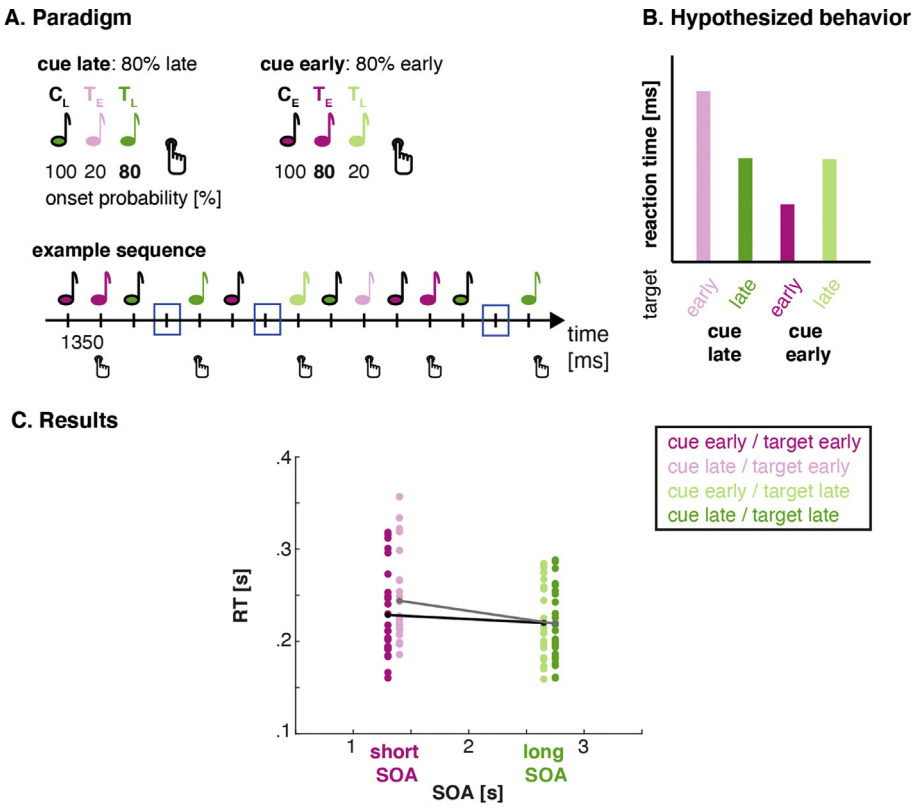

Fig. 1 – A. Study Design: Tone pairs were presented, forming a rhythmic stream. Each pair consisted of a cue (C, black contours), and a target (T, colored). Cues could be of two frequencies (1046 and 1318 Hz, indicated in pink and green), which were associated with the target's (1975 Hz) onset probability at the late (2700 msec, L) or early (1350 msec, E) time point following the cue, that is a with a 20% versus 80% or 80% versus 20% probability-ratio for a short versus long SOA. Participants were instructed to respond to the target with a button press as fast as possible. The lower panel depicts an example sequence with the time window of interest for the EEG analysis marked by blue squares. B. Hypothesized facilitation of reaction times by expectation: targets occurring at the expected time led to shortened reaction times (darker bars). The effect was hypothesized to be more pronounced at the early time point (depicted in pink). C. Results: As predicted, reaction times to targets occurring at the short SOA were faster when the cue indicated an early target versus a late target. At the long SOA, no statistically significant difference was found between valid and invalid cues.

2.3. *Behavioral analyses*

Reaction times were screened for outliers on single trials, defined as differing by more than three standard deviations from the participant's mean, and removed. On average, we removed 31.23 trials per participant (SD: 12.78).

To decide when to stop testing (referred to as **Hypothesis 1**) we performed a paired, one-sided Bayesian *t*-test on reaction times for targets occurring at the early time point, using the R-package *BayesFactor* (Morey & Rouder, 2018, decision criterion: BF >10 or BF< .1).

After completion of data collection, we computed a linear mixed effect model on single trial log-transformed reaction times, using the *lme4* package in R (Bates et al., 2015). We modelled target occurrence (early/late) and whether this matched the expectation (expected/unexpected) as fixed effect factors, plus their interaction. We specified random intercepts and random slopes for both factors and the interaction, allowing them to vary over participants. To compute *p*-values, we used the Satterthwaite approximation of degrees of freedom, implemented in the *lmerTest* package in R (Kuznetsova et al., 2016). The α level for assuming statistical significance is set to $p < .02$.

Hypothesis 1 was assessed by testing for a main effect of expectation on reaction times (reduced reaction times at expected time points). We also expected to find an interaction of expectation and target occurrence, such that the reduction of reaction times is more pronounced at the early time window.

2.4. *EEG recordings*

EEG was recorded with 64 electrodes from an Acticap (Easy Cap) system, with one of the electrodes attached to the nose [1], connected to an ActiChamp (Brain Products) amplifier using the software Brain Recorder (Brain Products). Impedance was kept below 10 kΩ. To retain the realised electrode localisation with good spatial specificity for posterity, we digitized each

[1] We did not use an external electrode as originally preregistered, because it was not compatible with the recording system.

participant's EEG electrode positions (using the Xensor system, ANT Neuro).

EEG data were recorded at 1000 Hz sampling rate, without an online high-pass filter (DC), and a low-pass filter of 300 Hz, contrary to the original study in which the recordings were performed with an .16–150 Hz analog high-pass filter.

After each recording, we recorded 3 min of EEG data with the same parameters as above, while participants listened to low-pass filtered white noise (5 kHz)[2]. To engage participants in listening, 6 target tones (the same as in the main task) were presented at random intervals during the 3 min. Participants were instructed to count the tones. These data were preprocessed as described below and used to test for spontaneous delta oscillations in auditory areas.

2.5. *EEG preprocessing*

For the preprocessing of the EEG data, we used the Fieldtrip software package (version 20200327, Oostenveld et al., 2011) for Matlab (version 2019a, MATLAB, 2019). The original study used the nose as reference. In accordance with our previous work, we re-referenced the data to linked mastoids using electrodes TP9 an TP10 from the cap. Furthermore, we also performed a comparison analysis with the data referenced to the nose electrode, as done by the original study.

In the original publication, a narrow delta-band filter, and a wide-band filter were applied to the data. Here, we produced four parallel versions of the data, by filtering the continuous data (before epoching) with different high- and low-pass filters. We chose not to apply a high-pass filter to the wide-band data to avoid temporal smearing, resulting from the long filters needed to achieve low high-pass cut-offs. To test how specific the phase coherence effect is in the frequency domain, we performed parallel analyses on data filtered for the low delta band (matching the stimulation frequency of .74 Hz), and for the theta band to test for a more broad-band effect that could also be influenced by evoked potentials.

1. Wide band, no high-pass filter: < 20 Hz
2. Delta band: .5–3 Hz
3. Low delta band: .25–1.5 Hz
4. Theta band: 4–7 Hz

All filters were causal (zero-phase) FIR filters, filtering in the forward and backward directions, using the firfilt routine implemented in Fieldtrip (Widmann et al., 2015). The analyses of phase consistency was performed on the delta band (2), low delta band (3), and theta band (4) version of the data. The analyses of the evoked responses were performed on the wide-band data (1) and the filtered versions (2–4).

Artifact rejection followed an established pipeline as used in previous studies (Herbst & Obleser, 2019), performed on the wide-band filtered data (<20 Hz), and applied to all other versions of the data. First, data were visually inspected to mark bad channels to be interpolated later. Then, the above filters were applied on the continuous data, before the data were be epoched from −500 msec before to 4050 msec after the cue stimuli. The epoched data were downsampled to 100 Hz to reduce computation time[3]. The wide-band filtered data were detrended over the whole epoch.

For the ICA, we produced an additional version of the continuous data, to which we applied a 1 Hz high-pass and a 20 Hz low-pass filter (same filter parameters as above)[4]. The 1 Hz high pass filter was added to make the ICA solutions more stable (Winkler et al., 2015), and to make the ICA blind to fluctuations at the stimulation frequency, in order to avoid having to make decisions about such components during the manual selection procedure.

ICA was then computed on epoched data, using the 'runica' algorithm. Components reflecting blinks, muscular artifacts, and unspecific noise occurring temporarily in a channel or trial were excluded, using the semi-automatic inspection of ICA components provided by the SASICA toolbox for fieldtrip (Chaumon et al., 2015) and removal of these, resulting in 2.19 (SD: .49) components removed on average per participant. Furthermore, we removed trials with voltage exceeding 100 μV [5] (on average 35.12 trials per participant, SD: 47.90) and inspected the remaining epochs visually to remove artefactual trials not detected by the above described procedure (4.58 trials on average, SD: 3.72).

After preprocessing, we retained on average 829.58 trials per participant (SD: 189.08).

2.6. *EEG analyses*

2.6.1. *Analysis of delta phase consistency using cosine similarity*

To assess instantaneous delta phase angles, we applied the Hilbert transform to the filtered and epoched data of the different filter bands, and extracted phase angles as the imaginary value of the complex Fourier spectrum [6]. The main analysis focuses on the delta band (.5–3 Hz), but all other narrow-band filtered versions of the data (see above) were run through the same procedure to assess the specificity of the effects.

The analysis of phase consistency was performed at the time of the expected delivery of the early target, 1350 msec following the cue (indicated by blue squares in Fig. 1A). We only included trials at which targets did not occur in this time window but at the later one, to keep the time window of interest free from target-evoked activity. In order to demonstrate the presence of ongoing oscillatory activity in a specific frequency range, we also display the phase-sorted single-trial data as done in the original study (Fig. 2).

[2] Originally, we had pre-registered to record 5 min, prior to the task and present 5 tones. Due to practical constraints, the block was shifted to the end of the session and shortened to 3 min.

[3] Resampling was missing in the pre-registration, but necessary to avoid too large data sets and computation times.

[4] Added after pre-registration.

[5] for one participant, the threshold was set to 150 μV, because of high-amplitude alpha oscillations, that would otherwise have resulted in rejecting many epochs.

[6] We had pre-registered to apply the Hilbert transform on the continuous data, before epoching, but realized that this would make the epochs-based artefact rejection procedure obsolete. Especially the resampling and rejection of ICA components led to transformations of the original data values, that would make the resulting phase angle time series difficult to interpret.

Inter-trial phase consistency (ITC), as most commonly computed, is not independent of the number of trials (Chou & Hsu, 2018), and tends to be inflated by small trial numbers. Given the design, comparing trials in which no target occurred at the early time point when the participant expected a target to occur then (20% of trials) versus at the second time point (80% of trials) leads to an important difference in the number of trials available per cue condition. Therefore, we computed cosine similarity instead of conventional ITC measures, separately per participant, condition, and electrode, which gives an unbiased and consistent estimate of phase consistency for finite sample size (Chou & Hsu, 2018).

The mean cosine angle of all given pairs of phase angles (*CS*) per condition was computed per participant as follows with n being the number of trials, and i, j = i+1, being the indices of single trials compared against each other:

$$CS = \frac{2}{n(n-1)} \sum_{i=1}^{n-1} \sum_{j=i+1}^{n} \cos(\theta_i - \theta_j) \quad (1)$$

To test for a statistically significant increase in phase consistency, we compared the obtained cosine similarity values per participant at electrode Cz (used in the original study), using the paired Bayesian *t*-test from the R-package *BayesFactor* (Morey & Rouder, 2018, one-sided decision criterion: BF > 10 or BF < .01). This test was used to decide when to stop testing (**Hypothesis 2**, p.5).

Hypothesis 2: In line with the original study, we expected to find increased delta phase consistency at electrode Cz when a strong (80%) versus weak (20%) expectation existed towards the early time point.

After completion of data collection, and confirmation of increased delta phase consistency at electrode Cz, we computed cosine similarity values for all electrodes and subjected them to a cluster-based permutation test (Maris & Oostenveld, 2007) at the group level. To assess differences in phase consistency between the early- and late-cue conditions, we computed a reference distribution of the difference between cue types using a permutation approach. To obtain the permutation distribution of the difference, we shuffled the cue types randomly over trials within each participant, keeping the ratio between numbers of early and late cues constant, and computed cosine similarity as above. This procedure was repeated 1,000 times [7]. The 98% percentile of the distribution of differences of phase concentration parameters between conditions was used as criterion to decide whether the difference in phase consistency between high and low expectation trials is different (directional test). Furthermore, the same analysis was computed on the low delta and theta band filtered data to assess the specificity of the effect to the delta range.

2.6.2. *Analysis of delta phase consistency using resultant vector length*

To match the analyses in the original study, and assess phase consistency of delta oscillations separately per condition, we computed phase concentration parameters as the resultant vector length *R* for all trials from one participant and condition (Berens, 2009):

$$R = \frac{abs\left(\sum_{n=1}^{N}(e^{i\cdot\theta})\right)}{N} \quad (2)$$

where θ denotes single trial phase angles in radian per condition and participant, *n* the number of trials from 1:*N*. To statistically test for phase alignment at electrodes Cz, Fz, Pz, C3, and C4, reflected by a non-random distribution of phase angles, we tested the distribution against a van Mises distribution, applying Rayleigh's test for uniformity of circular data, implemented in the *CircStat* package for Matlab (Berens, 2009; Fisher, 1995), for both cue types separately. We expected to see significant delta phase concentration ($p < .02$) in both cue conditions. As described for cosine similarity above, we also computed the resultant vector length *R* at all electrodes and compared it against a reference distribution obtained from permuting the cue conditions.

2.7. *Additional analyses*

2.7.1. *Separating oscillatory from 1/f activity*

The original study assessed the presence of entrained delta oscillations by computing fast Fourier spectra (FFT) of the interval −500:0 msec prior to target onset at electrode Cz. Here, we additionally assessed whether the activity observed in the delta band is truly oscillatory, rather than reflecting aperiodic 1/f activity. To this end, we applied the irregular resampling technique (IRASA, Wen & Liu, 2016; see also Helfrich et al., 2018; Henry et al., 2016; Herbst & Obleser, 2019) to the epoched data [8], as well as to the 3-min continuous noise recording (epoched into 5-sec segments to match the epoch duration of the task data). The IRASA technique consists in downsampling the data at pairwise non-integer values and computing the geometric mean of the resulting power spectra. The resampling leaves the 1/f activity intact but removes narrow-band oscillatory activity. Power spectral density (PSD) was computed on the epochs, padded to 5.4 sec, and in .19 sec steps (parameters chosen to include the stimulation frequency and multiples thereof in the resulting frequencies), using a fast Fourier transform tapered with a Hanning window for a frequency range of .19–22.2 Hz, without detrending, and the default resampling parameter for IRASA (1.1–1.9, .05 increment).

To assess the presence of oscillatory activity, we subtracted the power spectrum of the re-sampled data from the power spectrum of the original data, and computed a 98% confidence interval of the difference over participants using the t-statistic to test for residual oscillatory activity in the delta frequency range (.5–3 Hz).

To assess whether delta oscillations were present throughout the whole trial rather than resulting from periodically elicited evoked responses, we masked the 300 msec after each target onset, and computed the power spectrum again (see supplementary Figure 1).

[7] The originally preregistered 10,000 permutations turned out too computationally intensive for the cosine similarity computation.

[8] to be consistent with the delta phase analyses.

Hypothesis 3: Given the rhythmic stimulation applied, we assumed to see a significant and narrow peak in the power spectrum computed during blocks, which was expected at the stimulation frequency (.74 Hz), supposedly reflecting entrained oscillations.

2.7.2. *Evoked responses in the peri-stimulus time windows*

Evoked responses, such as the contingent negative variation (Walter et al., 1964) and P300 (Schürmann et al., 2001), have been described in relation to expectation, by a literature mainly separate from the one referring to neural oscillations. It is to date an open question, whether these responses relate to different or at least partially overlapping brain processes (Lakatos et al., 2008; Makeig et al., 2002). Answering this question from an empirical point of view likely requires an extended research program, including invasive recordings of local field potentials.

Nevertheless, we applied a set of additional analyses in the frequency and time-domain to better understand the nature of the observed effects. In the time domain, we assessed responses to cue and target tones, from the wide-band and narrow-band filtered data. Specifically, we compared the cue-evoked responses for cues predicting early versus late target onsets, and the target-evoked responses for expected versus unexpected targets at the early and late time point. Additionally, we compared the evoked responses in the time window of the early target onset, when no target occurred then, to assess omission responses and their modulation by the strength of the expectation.

To test for statistically significant differences in the time-domain data, we applied cluster permutation tests on two levels. First, we contrasted evoked activity for each stimulus and condition for each participant using independent samples regression implemented in FieldTrip (ft_timelockstatistics). The resulting regression coefficients (betas) for each time-electrode data point for the evoked responses were subjected to a group level analysis, using a dependent samples *t*-test to contrast the betas from the subject-level analysis against zero. A permutation test (5000 Monte Carlo random iterations) was performed with cluster-based control of type I error at a level of $\alpha = .02$.

As in the original study, we further performed a correlation analysis, to assess the overlap between evoked responses and delta phase consistency. To this end, we correlated the condition differences (expected vs unexpected) measured in the time domain (post-cue and post-target) with the potential phase-consistency effects. We also assessed the partial correlations of each of these measures with the reaction times, to disentangle their explanatory power. In addition to the Pearson correlation values and Bayes Factors, we report percentage bend correlation coefficients (beta = .2), as a robust measure of correlation (Pernet et al., 2013).

Hypothesis 4a: We expected to see a difference in early sensory evoked potentials between predicted and non-predicted targets. The existing literature is somewhat undecided with respect to the expected directions of the ERP differences (Lange, 2013), thus, we did not specify a direction here. In a previous experiment (Herbst & Obleser, 2019), we found a difference in target-evoked potentials, with a more negative N1/P2 component after predicted targets.

Hypothesis 4b: We expect to see an omission response at the time point of the early target onset, when no target occurred, with a larger amplitude on trials on which expectation was stronger. The strength of this response was expected to be partially correlated with pre-target delta phase consistency.

Hypothesis 4c: Correlation analyses were expected to show partial, but not full overlap between the time domain signatures of expectation and delta phase consistency.

2.7.3. *Source reconstruction*

Since we obtained a significant difference in delta phase consistency in sensor space we visualized the source distribution of delta phase consistency at the time point of the short SOA for trials in which no target occurred then. Compared to the pre-registered methods, the source reconstruction pipeline was subject to slight adjustments, validated on the reconstruction of delta and theta band phase coherence 300 msec after the cue and early target onset, where we expected strongly phase-locked auditory activity. This validation is independent from the comparison of interest. As it turns out, the cue evoked response is most strongly reflected by theta band phase coherence (see also Fig. 6).

We used the individually digitized electrode positions, combined with a standard MRI template, and a standard head model (based on the boundary-elements method) as implemented in FieldTrip (Oostenveld et al., 2003). The individual electrode positions were coregistered to the MRI template by first aligning the fiducials, and second, manually aligning the electrodes to the head surface. The delta-band filtered data was re-referenced to the average of all channels before computing each individual's lead field matrix using a 1-cm grid resolution. We then applied dynamic imaging of coherent sources (DICS, Gross et al., 2001) to construct the inverse model based on the cross spectral density computed from the Fourier transformations of the band-pass filtered data (−.5 to 4.5 sec), centred at the average frequency of the respective band. The dominant orientation per voxel was obtained using singular value decomposition. We then applied the precomputed filters to the analytic representation of the single trial data (obtained through the Hilbert transform) via matrix multiplication.

Cosine similarity was computed on single voxels, to visualize the distribution of delta phase consistency per condition. We computed a *t*-test between cues indicating early versus late targets, using the Montecarlo permutation method (ft_sourcestatistics). Since the source reconstruction was performed to localize the findings at the sensor level and not as an independent statistical test, we display the T-values thresholded at, $p < .02$ (non-parametric permutation test) without any further correction for multiple comparison (Fig. 2D, H). Source labels are reported based on the AAL atlas (Tzourio-Mazoyer et al., 2002).

While we have shown in previous work that auditory and motor-like sources can be broadly distinguished by reconstructing source activity from EEG data (Herbst et al., 2018), the identification of the exact anatomical generators will require further confirmation by follow-up studies, for instance using MEG.

Hypothesis 5: We expected to see the strongest delta phase consistency in auditory and motor areas (Morillon et al., 2019; Morillon & Baillet, 2017).

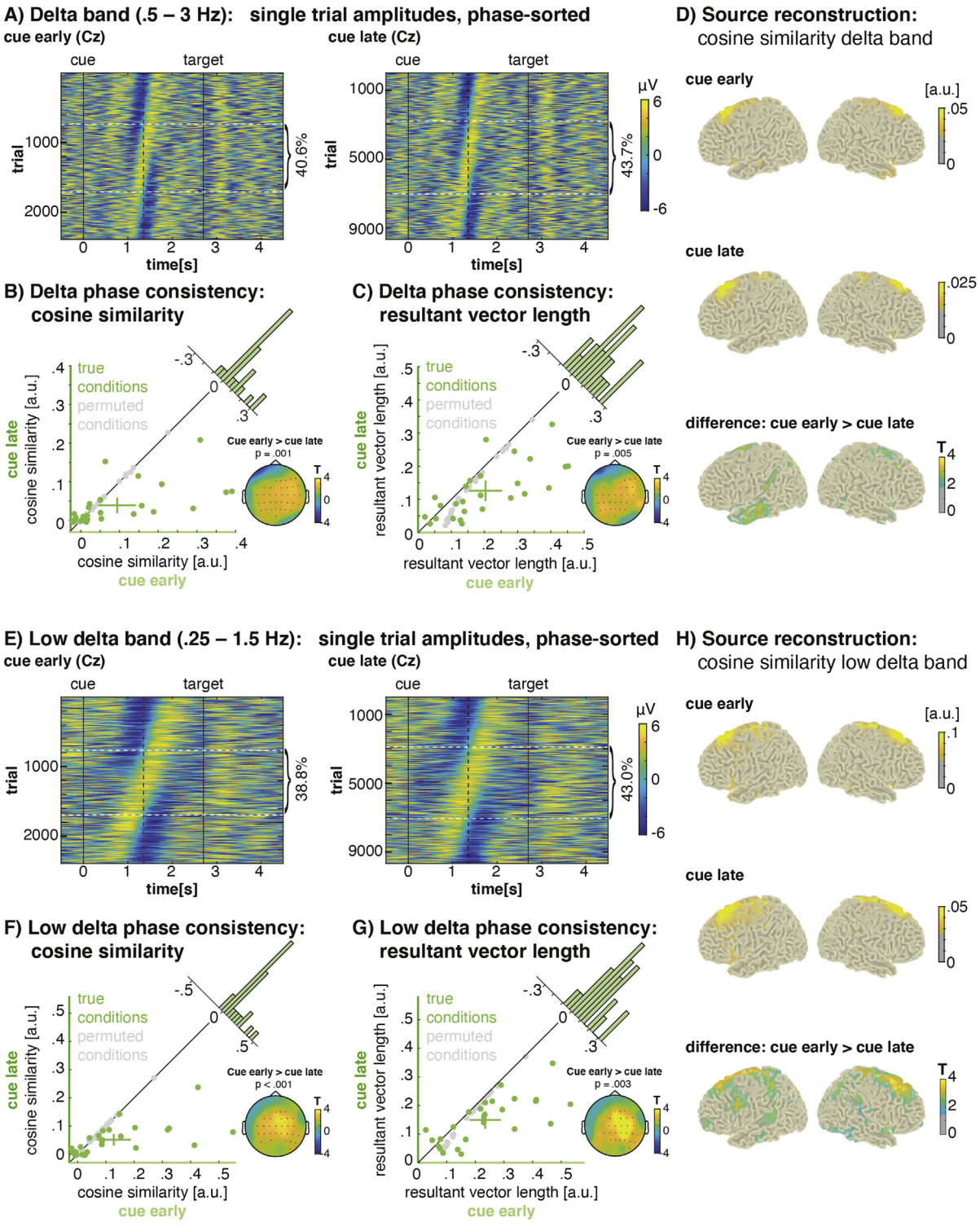

Fig. 2 – A. Delta band (.5–3 Hz), phase-sorted amplitude time courses: This display was included for better comparison with the original study (their Fig. 3E and F) and shows all trials of all participants, for the long SOA, with cues indicating an early target in the left panel, and cues indicating a late target in the right panel. The band-pass filtered single trials were sorted by phase angle at the early SOA. The range between the horizontal white lines, demarcating phase angles between $-\pi/2$ and $\pi/2$, is considered the less favourable phase. The proportion of trials in that phase range is smaller in the cue early condition (40.6%), compared to the cue late condition (43.7%). B. Delta phase consistency, cosine similarity: Phase consistency was higher in the cue early condition, indicated by most green dots lying beyond the diagonal line. Grey dots depict phase consistency values computed after permuting trials randomly between conditions. The topography shows the significant cluster when comparing phase consistency between the true conditions and the resampled version. The histogram above the diagonal depicts the differences cue early – cue late. C. Delta phase consistency, resultant vector length: As in B, but

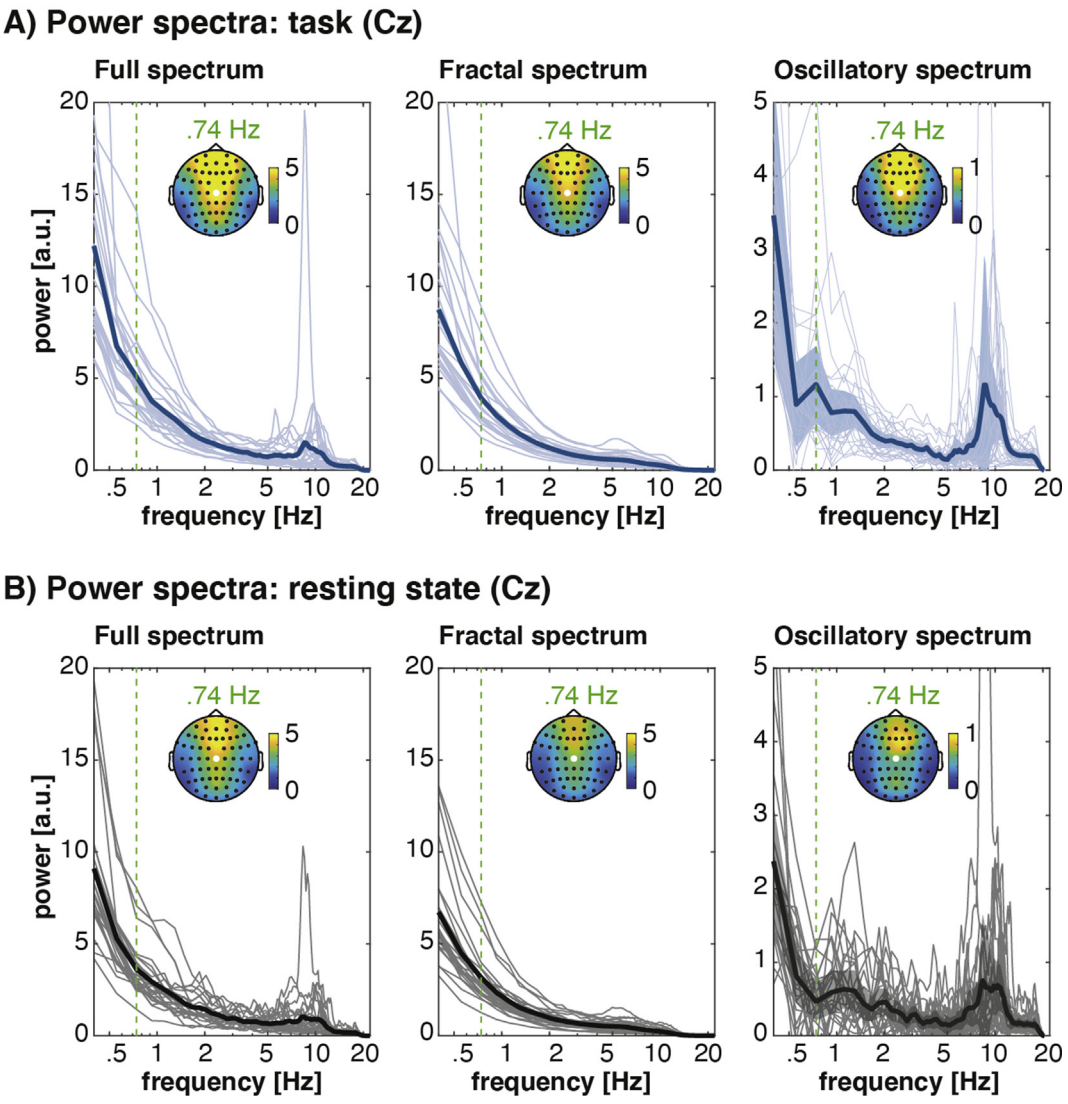

Fig. 3 – Power Spectra. A) Power spectra of the task data, all at electrode Cz. Left: Full power spectrum. Middle: Fractal power spectrum, computed using the irregular resampling technique. Right: Oscillatory spectrum, computed as the difference between the full and fractal spectra. Thick lines depict participant average, thin lines single participants' spectra. The blue shade in the right panel depicts the 98% confidence interval. The green dotted vertical line indicates the stimulation frequency (.74 Hz). The topographies show the scalp distribution of power at .74 Hz. B) Power spectra of the resting state. Panels: as in A. While the power spectra computed on the task data showed a peak at the stimulation frequency, the resting state data did not show a clear peak.

here phase consistency was measured by resultant vector length. The departure of the grey dots from the diagonal indicates a systematic overestimation of phase consistency by this measure for the condition with fewer trials. Nevertheless, the comparison between true and permuted conditions showed a significant cluster. D. Source reconstruction. Average cosine similarity values at the short SOA are shown overlaid on a template brain, for cue early and cue late conditions separately (note the different color scales). The third panel shows the difference between cue early and cue late with the colors scale indicating T-values thresholded at $p < .02$ (non-parametric permutation test) with no further correction for multiple comparisons. In the delta band, the difference in phase-locking was strongest in temporal (auditory) areas, as well as pre-motor and motor areas. E–H: Low delta band (.25–1.5 Hz). Same as A–D, but for the low delta band. Phase consistency in the low delta band was significantly higher after cues indicating an early versus late target, with a pattern very similar to the results observed in the delta band. In source space, the difference was most pronounced in pre-motor and motor areas, but also occurred in temporal and parietal areas.

Table 1 – Statistical results of the reaction time analysis. A linear mixed effect model revealed significant main effects of cue validity and SOA, as well as a significant interaction.

	F value	*p* value
cue validity	F (1, 24.97) = 28.80	< .001
SOA	F (1, 24.98) = 14.64	< .001
cue validity × SOA	F (1, 24.89) = 20.92	< .001

3. Results

3.1. *Expectations speed up reaction times*

In line with Hypothesis 1, reaction times were affected by the predictions conveyed by the cues (see Fig. 1). At the short SOA, responses to validly cued targets were faster than responses to invalidly cued targets (valid: .229 sec, SD = .048 sec, invalid: .244 sec, SD = .046 sec; significant difference: t (25) = 5.42, p < .001, Bayes Factor (BF) = 3464.96; one-sided tests performed on log-transformed reaction times). Furthermore, we found the hypothesized interaction, namely no significant difference in reaction times at the long SOA (validly cued: .219 sec, SD = .039 sec, invalidly cued: .220 sec, SD = .039 sec; t (25) = 1.28, p = .11, BF = .76).

The linear mixed effect model computed on single trial log transformed reaction times confirmed that both factors, SOA and cue validity were significant, as well as their interaction (see Table 1).

3.2. *Delta phase consistency increases with expectation for target occurrence*

In confirmation of Hypothesis 2, we observed increased delta phase coherence at electrode Cz at the time point of the early SOA when the cue predicted an early versus a late target (cosine similarity, cue early: .09, cue late, .04, T (25) = 2.67, p = .006, BF = 7.40). In the low delta band, the effect was even stronger, as indicated by the larger absolute difference and Bayes Factor (cosine similarity, cue early: .13, cue late, .05, T (25) = 2.30, p = .003, BF = 14.37).

The phase-sorted single trial amplitude time courses depicted in Fig. 2A and E (displayed to match the original study) show that across all participants 40.6% of cue early trials had a delta phase angle of $-\pi/2$ and $\pi/2$ at the early SOA, considered the less favourable phase, versus 43.7% in the cue late condition (38.8% vs 43.0% for the low delta band).

Cluster permutation tests comparing the difference in cosine similarity between cue early and cue late trials at all electrodes against the difference obtained from permuting trials between the two conditions revealed significantly increased phase consistency in the delta and low delta bands, but not in the theta band (see Fig. 2, statistics reported in Table 2). The analysis of resultant vector length found similar results.

The cluster permutation analysis takes into account the difference in the number of trials per condition (cue early: 20%, cue late: 80%), as the trial numbers were kept consistent when computing the permuted differences. As can be seen in Fig. 2 B, D (and panels F, G, for the low delta band), cosine similarity was not inflated for the condition with fewer trials (the grey dots indicating the permuted difference lie on the unity line), while for resultant vector length there was an inflation (grey dots lie beyond the unity line).

We performed a control analysis with the nose electrode as the reference to match the original study, which yielded a weaker increase in phase consistency for the cue early condition (delta band: cosine similarity, cue early: .08, cue late, .04, T (25) = 2.02, p = .027, BF = 2.31; low delta band: cosine similarity, cue early: .16, cue late, .06, T (25) = 3.60, p = .004, BF = 12.26). The decrease in effect size might be explained by the fact that the recording from the nose electrode turned out to be rather noisy in many participants.

Source reconstruction of delta and low delta phase consistency (cosine similarity; Fig. 2 D, H) showed mainly premotor and motor sources, extending into frontal areas, as well as anterior temporal and auditory areas. In the delta band, the difference between the cue-conditions was most apparent in temporal areas (middle and inferior temporal gyrus, predominantly in the left hemisphere), and somewhat weaker in (pre-)motor areas (right supplementary motor area). In the low delta band, the strongest difference occurred in (pre-)motor areas (supplementary motor areas, stronger in the right hemisphere), extending into frontal areas. Weaker differences were observed in parietal and temporal areas.

In line with the original study, we also tested whether the phase distributions in the delta band were randomly distributed or concentrated, as a signature of entrainment. Significant delta phase concentration at the early SOA was observed at electrode Cz in 13 out of 26 participants for the cue early condition, and 18 participants in the cue late condition (*p*-values < .02; Fz: 10/14, C3: 12/15, Pz: 10/12, C4: 12/14). For the low delta band, 17 participants had a significant phase

Table 2 – Statistical results of the phase consistency analyses. The average phase consistency across participants is reported for the two measures: cosine similarity and resultant vector length, both for electrode Cz. Cluster permutation tests comparing the difference in phase consistency between cue early and cue late trials at all electrodes against the difference obtained from permuting trials between the two conditions revealed significantly increased phase consistency in the low delta and delta band for both measures, but not in the theta band.

frequency		mean (Cz) cue early	mean (Cz) cue late	cluster *p*-value
low delta	cosine similarity	.13	.05	p < .001
	resultant vector length	.23	.15	p = .003
delta	cosine similarity	.09	.04	p = .001
	resultant vector length	.20	.13	p = .005
theta	cosine similarity	−.01	.01	no positive cluster found
	resultant vector length	.08	.05	no positive cluster found

concentration at electrode Cz in the cue early and 20 in the cue late condition (p-values < .02; Fz: 15/14, C3: 13/20, Pz: 15/21, C4: 18/16). These results suggest oscillatory entrainment in the majority, but not in all participants.

Additionally (not part of the pre-registration), we visualized phase locking values over time for the two SOAs and two cue conditions, for the delta, low delta, and theta band (see Fig. 6). Interestingly, delta and low delta phase consistency showed a transient increase after targets, but much less after cues, while evoked responses at the cue and target led to a prominent increase in theta phase consistency. A prolonged difference at the early SOA between cues indicating early versus late targets (green lines) occurred in the delta and low delta band, as already apparent in the previous results.

3.3. *Power spectra show peaks at the stimulation frequency*

We assessed the power spectra of the data recorded during the task and the subsequent block in which participants listened to white noise (Fig. 3). After removal of the 1/f slope, the oscillatory spectrum contained a peak at the stimulation frequency (.74 Hz) at fronto-central electrodes in the task data Fig. 3A), but not in the resting state data Fig. 3B). The peak indicates an oscillation evoked by the rhythmic stimulation, and confirms Hypothesis 3. Note that the seemingly larger rise at around .3–.4 Hz reflects the cut-off in the power spectrum caused by the epoch duration (5 sec), preventing us from computing power at the lowest frequencies.

After removing the target-evoked responses (0–300 msec after each target), power spectra still showed a peak at the stimulation frequency, albeit with slightly reduced power (shown in Supplementary Figure 1).

3.4. *Evoked responses show stronger pre-target deflections towards predicted early targets, and post-target differences in the delta band*

We observed clear auditory evoked responses to cue and target tones, as well as a negative deflection following the cue (see Fig. 4). In the long SOA trials, a delta-like wave form was observed at central electrodes.

Contrary to Hypothesis 4a, we observed no statistically significant differences in the evoked responses to expected and unexpected targets in the wide-band data (0–20 Hz, Fig. 4A, see also Table 3). In the delta-band filtered data (.5–3 Hz, Fig. 4B), we observed a stronger response to expected early targets (cue early) compared to unexpected early targets (cue late; 1.48–1.84 sec, $p < .01$). No significant effects were found for the late target trials ($p < .14$).

As specified in Hypothesis 4b, we expected to see an omission response in trials for which the cue predicted an early target but none appeared, defined as an evoked-like potential in the post-target window (Dercksen et al., 2020; SanMiguel et al., 2013). No such response was observed, neither in the wide-band nor the delta-band data.

However, the cue-evoked responses were indicative of the prediction conveyed by the cue: in the wide band data, we observed a more negative-going slow wave towards the early SOA when the cue predicted an early target (early target trials: 1.20–1.37 sec, $p < .01$; marginal for the late target trials: 1.16–1.29 sec, $p = .03$). In the delta-band data, the post-cue difference was not significant (early target trials: 1.19–1.4 sec, $p = .079$).

Evoked responses in the low delta band and theta band data showed no significant differences (low delta $p > .06$; theta $p > .03$).

3.5. *Reaction time facilitation by valid cues correlates with delta phase consistency*

We tested for correlations of the reaction time facilitation by valid cues and the difference in delta phase consistency (and evoked responses, respectively) across participants (see Table 4 and Fig. 5).

The difference in log-transformed reaction times at the short SOA correlated significantly (albeit only marginally for the robust correlations) with the difference in delta phase consistency (cosine similarity) measured at the short SOA (taken from the long SOA trials as in the previous analyses, electrode Cz; $\rho = -.56$, robust correlation $-.29$). In the low delta band, the correlation was significant, too ($\rho = -.56$, robust correlation $-.56$), see Fig. 5A). The negative correlation indicates that participants who showed greater reaction time benefits from valid cues at the early SOA also had stronger delta phase consistency around the early SOA when the cue predicted an early versus late target.

The reaction time facilitation did not significantly correlate with the observed differences in the slow negative potentials following the cue (wide-band data, 1.20–1.37 sec post-cue, $\rho = .27$, Fig. 5B, left). However, we observed a correlation between the difference in reaction times and the difference in the delta band evoked response at the early target (1.48–1.84 post-cue, $\rho = -.63$, robust correlation $-.71$, Fig. 5B, right), indicating that participants who responded faster to validly compared to invalidly cued targets also showed larger differences in the evoked response to those targets.

No significant correlations were observed between the differences in delta phase consistency and evoked responses (Fig. 5C).

We also computed partial correlations between the differences in reaction times, the differences in delta phase consistency, and differences in the evoked response (slow negativity observed in the wide-band data). When controlling for the evoked response, the correlation between phase consistency and reaction times dropped to $\rho = -.39$ ($p = .05$). When controlling for phase consistency, the correlation between the evoked response and reaction times dropped to $\rho = .23$ ($p = .28$). It is important to mention here that the reaction times and evoked responses were both taken from short SOA trials, while the cosine similarity measures were computed from long SOA trials.

The original study reported correlations between the phase of the delta oscillation at target onset with reaction times, as well as the latency and peak amplitude of the P300 component of the evoked response, taken from single trials in Experiment 1 (slightly different experimental design). All measures were

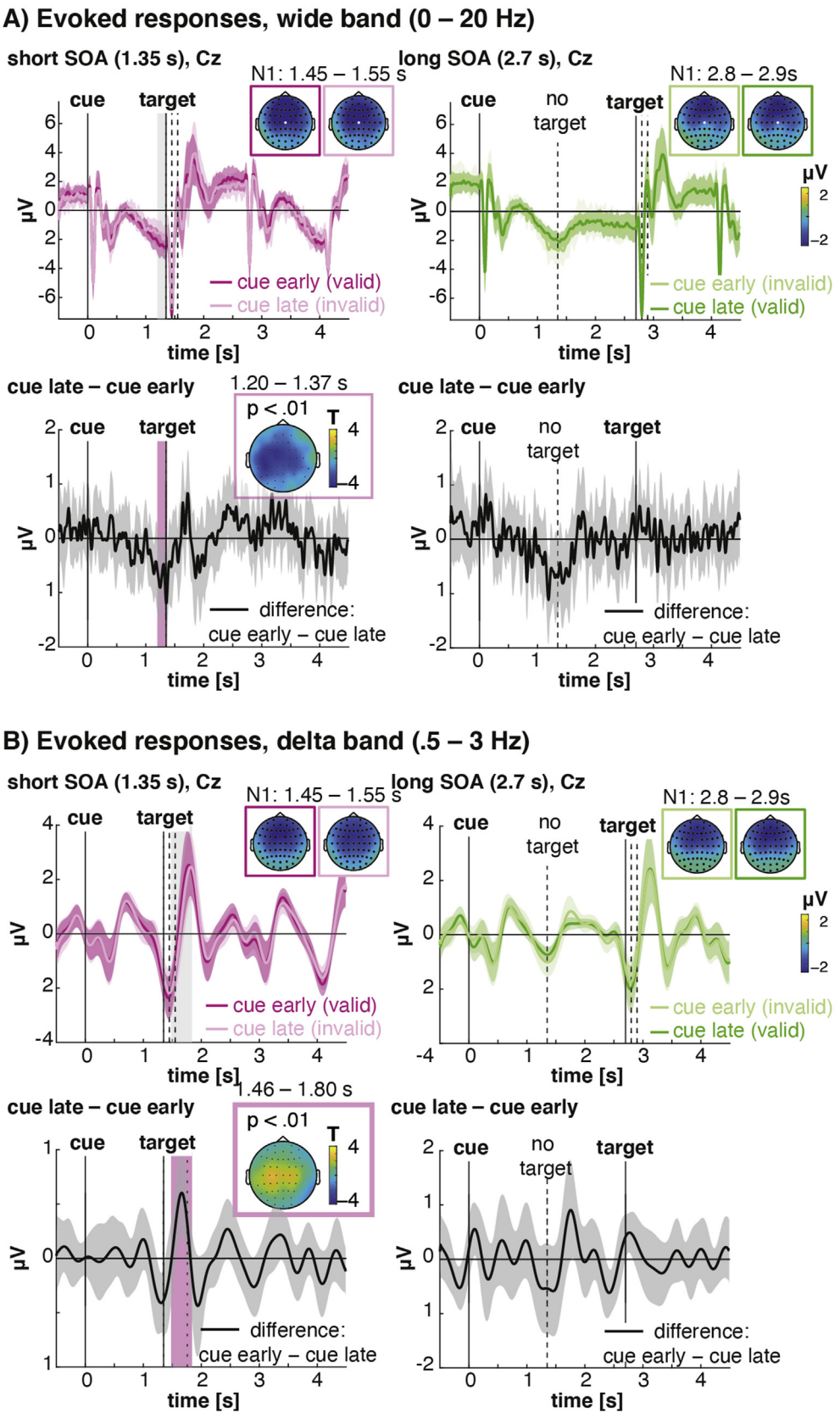

Fig. 4 – A. Evoked responses, wide band: Average evoked responses, time-locked to the cue at electrode Cz. Top, left: short SOA (1.35 sec). Activity evoked by cues predicting early targets (valid, dark pink) versus cues predicting late targets (invalid, light pink). Top, right: long SOA (2.7 sec). Activity evoked by cues predicting early targets (invalid, light green) versus cues predicting late targets (valid, dark green). The topographies show activity in the N1 time window, 100–200 msec after the

Table 3 – Statistical results of the evoked response analysis. Findings are reported per filter band and SOA at which the target was presented. The latencies indicate the duration of the significant clusters time-locked to the cue. As for the direction, 'neg' means that the evoked activity was smaller (or more negative) following cues which predicted an early compared to late target. For 'pos' the direction is reversed.

filter	SOA	latencies	direction	cluster *p*-value
wide band	1.35 sec	1.20–1.37 sec	neg	$p < .01$
	2.7 sec	1.16–1.29 sec	neg	$p = .03$
delta band	1.35 sec	1.48–1.84 sec	pos	$p < .01$
	2.7 sec	1.19–1.4 sec	neg	$p = .08$
low delta band	1.35 sec	1.02–1.39 sec	neg	$p = .06$
theta band	1.35 sec	.99–1.04 sec	pos	$p = .09$

Table 4 – Statistical results of the correlation analyses. All tests are one-sided. The ρ and *p*-values in brackets indicate percentage bend correlation coefficients, a robust correlation estimate.

variables	ρ	T value	*p*-value	Bayes Factor
RT/ cosine similarity (delta)	−.56(−.29)	T (24) = − 3.32	.001 (.08)	32.65
RT/ cosine similarity (low delta)	−.56(−.56)	T (24) = − 3.35	.001 (.001)	34.81
RT/ evoked response (post-cue, wide band)	.28 (.11)	T (24) = 1.43	.08 (.30)	1.68
RT/ evoked response (post-target, delta band)	−.63(−.71)	T (24) = − 4.00	< .001 (< .001)	117.01
cosine similarity (delta)/ evoked response (post-cue, wide band)	−.244(−.14)	T (24) = − 1.23	.11 (.25)	1.33
cosine similarity (low delta)/ evoked response (post-cue, wide band	−.37(−.16)	T (24) = − 1.98	.03 (.22)	3.53
cosine similarity (delta)/ evoked response (post-target, delta band)	.18 (.09)	T (24) = .87	.20 (.33)	.90

taken at the same SOA and from single trials. Here, we computed correlations between the differences in the respective measures and at different SOA, which might explain why we did not find consistent correlations between phase consistency and evoked responses.

4. Discussion

In this study, we set out to replicate the seminal findings reported by Stefanics et al. (2010, Experiment II), namely an increase in phase consistency of the delta oscillation with the expectation for a target onset in the upcoming cycle of an ongoing rhythm. All major findings of the original study were replicated. We found a consistent reduction of reaction times following validly cued versus invalidly cued early targets by about 15 msec, confirming Hypothesis 1 (see also Fig. 1). A robust effect of increased delta phase consistency with expectation was observed, confirming Hypothesis 2 (see also Fig. 2). Additional analyses suggest that the increase in phase consistency results from oscillatory entrainment rather than reflecting an evoked response.

Concerning the more exploratory hypotheses spelled out in the pre-registration, we observed a spectral peak at the stimulation frequency (Hypothesis 3, Fig. 3), and sources for the phase consistency difference predominantly in premotor, motor, and in temporal areas (Fig. 2). The findings for the evoked responses did not adhere fully to the spelled out hypotheses: no post-target differences were observed in the wide-band data with respect to expectancy (Hypothesis 4a), but a stronger response to expected targets was observed in the narrow-band delta evoked response (Fig. 4). Furthermore, we observed, in the time window following the cue, a stronger negative CNV-like deflection when the cue predicted an early target (Mento, 2013; Praamstra et al., 2006). However, no omission response was observed in the time window following unexpected omissions of the early target (Hypothesis 4 b). Brain-behavior correlations were observed between reaction times and delta phase consistency, as well as responses evoked by early targets (Hypothesis 5).

target onset (indicated by the vertical dashed lines). Bottom row: Differences between early and late cues for the early (left) and late SOA trials (right). In the early-SOA trials, a significantly more negative potential was observed following cues predicting an early target. The pink shade indicates the time window in which a significant difference was found between the two conditions, accompanied by the topography of the statistically significant cluster. A similar pattern was found for the long SOA trials, but the difference was not statistically significant. Strictly speaking, the observed pre-target difference does not confirm the original Hypothesis 4a, which predicted *post-target* differences in the broad band data. B. Evoked responses, delta band: Same as in A, but for the delta-band filtered data. A larger target-evoked response occurred after expected versus unexpected early targets (left column). No differences were found in the pre-target window.

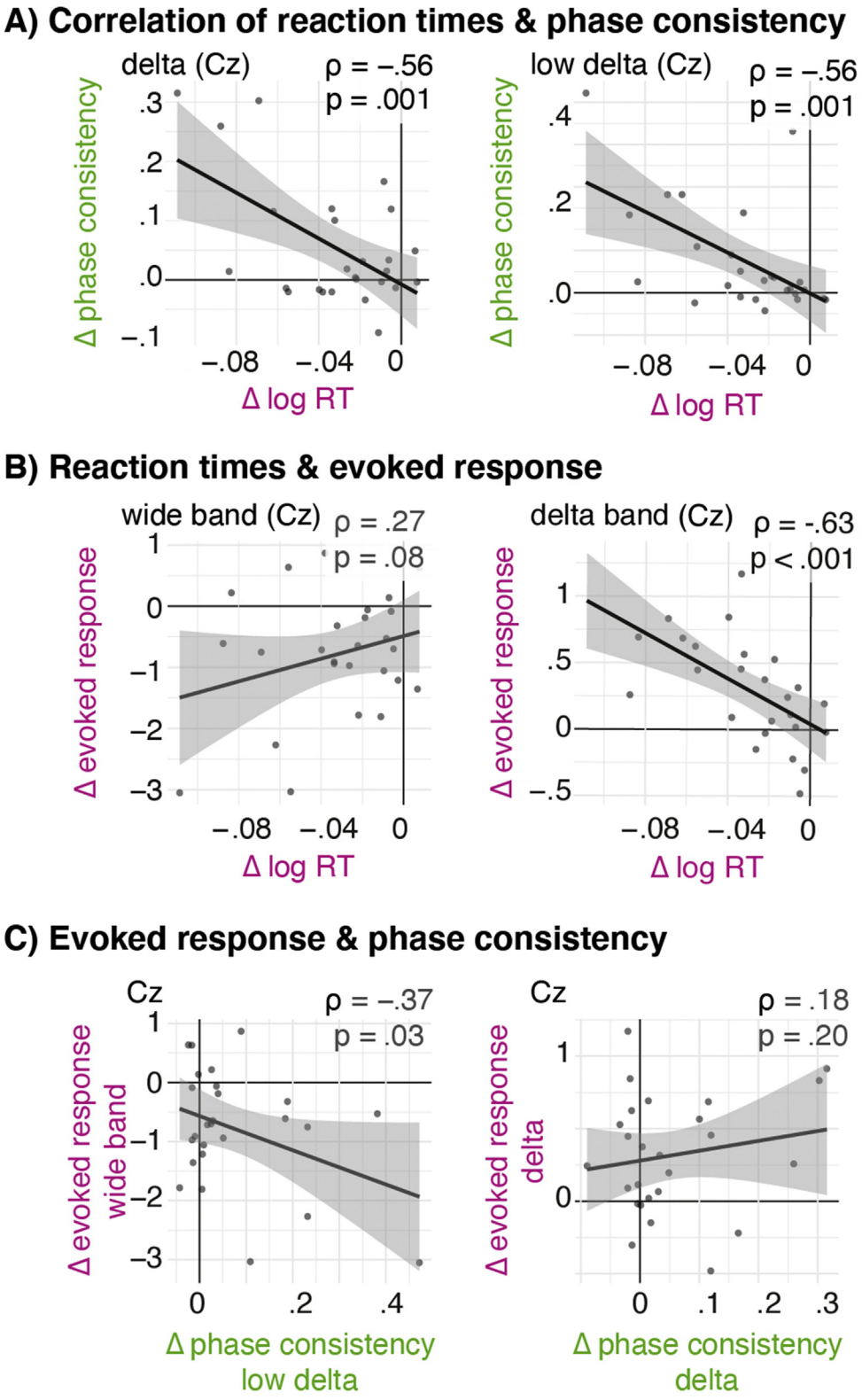

Fig. 5 – Brain-behaviour correlations. A) Correlation between reaction times and phase consistency for the delta band (left) and low delta band (right). Participants who had a larger difference in reaction times after expected versus unexpected early targets also had a larger difference in cosine similarity at the early SOA following early versus late cues. B) Correlation between reaction times and evoked responses. No significant correlation was observed between reaction times and the difference in the post-cue negativity observed in the wide band data (1.20–1.37 sec post-cue, right panel). Participants who had a larger distance in reaction times also had a larger difference in the delta-band evoked responses to expected versus unexpected early targets (1.48–1.84 post-cue, left panel). C) Correlation between evoked responses and phase consistency

4.1. Oscillatory phase locking as a mechanism for prediction

Importantly, the replication, in line with the original study, shows that delta oscillatory phase is under endogenous or top-down control, allowing for an increase in phase consistency with an expectation set by the preceding cue (80% versus 20% probability for target occurrence, see also Fig. 2). The correlations observed between reaction times and phase consistency further underline the behavioral relevance of the phase locking (Fig. 5A). Together, these findings strengthen the cognitive role of phase entrainment as a means to align slow neural oscillations to external temporal regularities to enhance the processing of task-relevant inputs (Arnal & Giraud, 2012; Jones, 2018; Schroeder & Lakatos, 2009).

With the increasing popularity of the theory of entrainment, criticisms have also emerged. In particular, a crucial premise for entrainment in the narrow sense is the existence of an endogenous oscillation that is entrained by exogenous inputs (Lakatos et al., 2019; Obleser & Kayser, 2019). Opposing views suggest that the observed phase consistency, at least in some studies, could be conflated with stimulus evoked responses occurring *after* the sensory event (van Diepen & Mazaheri, 2018; Zoefel & Heil, 2013), rather than oscillatory phase locking in anticipation of the stimulus. Especially for low frequent oscillations, this distinction is difficult to make due to signal processing constraints (for successful examples see the review by Zoefel et al., 2018).

Here, we conducted several additional analyses, which in our view support the interpretation of the effects as oscillatory phase locking, rather than an evoked response. First, delta phase consistency at the expected target onset increased in a narrow frequency band, most strongly in the low delta band which captured the ongoing rhythmic stimulation (.74 Hz), as well as the delta band, but not in the theta band. The frequency-specificity strengthens the proposed role of delta phase for endogenous predictions (see also Saleh et al., 2010). The phase-locking time courses for the three bands (depicted in Fig. 6) further emphasize this point: delta and low delta phase consistency was consistently increased throughout the trial in line with an oscillation and increased transiently only after targets, while theta phase consistency increased transiently after all auditory events, likely capturing the evoked response.

Second, we observed a peak at the stimulation frequency in the power spectrum after removing the 1/f activity (Fig. 3), further supporting an oscillatory response. Interestingly, the oscillatory power spectra during rest also show a rather broad peak around 1–1.5 Hz, which could be indicative of spontaneous oscillations in the delta band serving as the basis for entrainment (Morillon et al., 2019). Further research will be needed to assess whether those peaks reflect spontaneous oscillations versus artefactual activity such as the heart beat.

Third, as to the overlap between evoked responses and delta phase consistency, the picture remains somewhat unclear. We did observe a pre-target difference in the wide-band data, interpretable as a stronger contingent negative variation (CNV) towards early and expected targets (Fig. 4A). However, we did not observe a significant correlation between this difference and the reaction times or the delta phase consistency effect (correlations remain inconclusive as indicated by the Bayes Factors; see also Fig. 5B and C, left panels). We also did not observe any significant omission responses at the time point of an expected early target (Dercksen et al., 2020; SanMiguel et al., 2013), ruling out that the increased phase consistency observed at this moment reflects a transient evoked response.

The post-target difference in the delta band evoked response did correlate with reaction times (Figs. 4B and 5B, C, right panels), but not with the delta band consistency effect (both measures came from different sets of trials, namely short and long SOAs, respectively). Overall, the difference in neural dynamics with respect to expectation seems best captured by the phase of a narrow-band oscillation matching the frequency of the stimulation.

Admittedly, the present design cannot fully disentangle whether the delta oscillation whose phase locks to the stimulation is an a-priori existing endogenous oscillation, or an oscillation that emerges in response to the rhythmic stimulation. We observed an oscillatory peak during the rhythmic stimulation, but not during a block in which participants listened to white noise without rhythmic stimulation (Fig. 3), suggesting that the oscillation emerged in response to the rhythmic stimulation. Even though the propensity of neuronal assemblies to spontaneously oscillate in the delta frequency range has been shown with intra-cranial recordings (Buzsáki & Draguhn, 2004; Halgren et al., 2018; Lakatos et al., 2005; Neymotin et al., 2021), this proof is difficult to achieve with non-invasive M/EEG recordings. In order to test whether the implementation of predictions through phase locking occurs specifically in the delta band or could occur in a wide range of frequencies, future studies could vary the stimulation frequency (see Zalta et al., 2020, for a behavioral paradigm), or include longer periods of stimulus omissions to test for the continuity of an endogenous oscillation (Saberi & Hickok, 2021; Zoefel et al., 2018).

The increase in delta phase consistency with an endogenous expectation is an important argument for an active role of neural oscillations in tracking and anticipating rhythmic sensory inputs. By entraining in period and phase to an external input, neural oscillations can implement temporal predictions, allowing to align brain states beneficial for the processing of the respective inputs with the predicted onsets (Arnal & Giraud, 2012; Jones, 2018; Schroeder & Lakatos, 2009). Given the strictly periodic stimulus sequence used here, there are two possible interpretations for the nature of the expectation: it could either be *temporal*, directed to the most likely time point of target occurrence, or *probabilistic*, directed to the first or second cycle of an externally driven oscillator whose period mechanistically defines the cycle duration. To further examine whether neural oscillations implement temporal predictions, variations of the period of the stimulation are necessary.

for the delta band. No significant correlation was observed, neither between the slow negative difference in the wide-band data and delta phase coherence (left panel), nor between the post-target difference in the delta band data and delta phase coherence. The colors of the axis labels indicate whether the measure was taken from short (pink) or long SOA (green) trials.

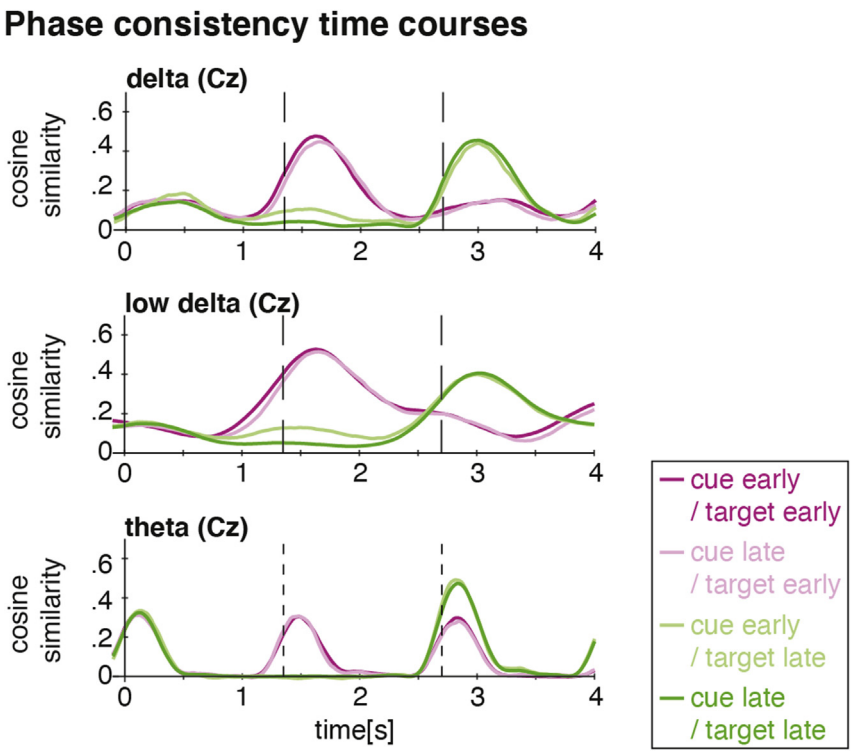

Fig. 6 – Phase consistency time courses per SOA and cue condition. Top: delta band, middle: low delta band, bottom: theta band. Targets led to transient post-stimulus increases in phase consistency in the delta, low delta, and theta bands, but only the theta band shows a substantial increase in phase consistency following the cue. Only the delta and low delta band show a prolonged increase in phase consistency in line with an oscillatory response, and a difference at the early SOA between cues indicating early versus late targets (green lines). The time points of possible target onsets (short and long SOA) are indicated by the vertical dashed lines.

Another open question is how much divergence from isochrony an oscillatory implementation of temporal prediction can afford (see also Obleser et al., 2017). While slight variations in the period have shown to be accounted for (Cannon, 2021; Doelling & Assaneo, 2021; Herrmann et al., 2016; Lakatos et al., 2013), recent research suggests that temporal predictions based on single intervals might rely on at least partially diverging mechanisms (Bouwer et al., 2020; Herbst & Obleser, 2017, 2019; Lange, 2013).

4.2. *Novel aspects of the current study*

We reconstructed the sources of the delta phase consistency effects, found to be predominantly in (pre-)motor areas, but also in parietal and temporal (anterior temporal and auditory) areas (Fig. 2), which is in line with Hypothesis 5. Interestingly, the difference in the delta band was stronger in the temporal and somewhat in parietal areas, while the difference in the low delta band (most specific to the stimulation frequency) was strongest in pre-motor and motor areas, extending into frontal and parietal areas.

This dominant localization of delta phase locking to (pre-) motor areas is in line with the assumption that rhythmic activity emerging from motor areas entrains auditory cortices to rhythmic inputs (based on Morillon & Baillet, 2017; Rimmele et al., 2018). However, we would like to mention that the strongly time-locked activity in bilateral auditory areas might pose a challenge for source reconstruction notably when using beamformers (Hincapié et al., 2017; Popov et al., 2018). In combination with the limited spatial resolution of EEG, this might have led to an under-representation of the auditory sources here. Follow-up studies using MEG could provide additional insights on the precise location of the anatomical generators.

In the low delta band, weak effects were observed in parietal regions, suggested to play a role in attentional processing more generally, and temporal prediction in particular (Besle et al., 2011; Coull et al., 2013). The difference to previous studies here probably results from the rhythmic paradigm (Coull et al.: interval-based predictions), and the reduced spatial resolution of EEG compared to functional magnetic resonance imaging (fMRI) and electrocorticography (ECoG in Besle et al., 2011).

An important methodological aspect of the study is that by design, conditions with 20% versus 80% of trials are compared, as a consequence of the manipulation of cue validity. This imbalance is particularly important when comparing phase consistency between conditions, as the commonly used measures for phase locking across trials (Bruns, 2004; Lachaux et al., 1999; Tallon-Baudry et al., 1996) have shown to be inflated for small number of trials (Cohen, 2014; Edwards et al., 2009). In this replication, we computed cosine similarity (Chou & Hsu, 2018), confirming its interpretation as an unbiased alternative to measure phase

locking. This is particularly apparent in the bias observed in the measure of resultant vector length towards the condition with fewer trials after permutation (indicated by the grey dots in 2C, G), which we did not see in cosine similarity (Fig. 2B, F).

5. Conclusions

In sum, we successfully replicated the original study, most importantly the modulation of delta phase consistency by endogenous expectations. Our additional analyses support the interpretation as an oscillatory effect, rather than a transient evoked response. Importantly, this work shows that the phase of delta oscillations is under endogenous control, and hence qualifies as a possible mechanism for the neural implementation of (rhythmic) temporal predictions.

CRediT authors statement

Sophie K. Herbst: Conceptualization, Methodology, Software, Validation, Formal analysis, Resources, Data curation, Writing–Original Draft & Review, Visualization, Supervision, Project administration, Funding acquisition.

Gabor Stefanics: Conceptualization, Methodology, Validation, Writing–Review.

Jonas Obleser: Conceptualization, Methodology, Validation, Resources, Writing–Review, Supervision, Project administration, Funding acquisition.

Open practices

The study in this article earned Open Data, Open Materials and Preregistered badges for transparent practices. Data for this study is available at https://osf.io/u24tn/.

Acknowledgements

The authors would like to thank Anne Herrmann, Franziska Scharata, and Martin Orf for help with setting up the experimental protocol and conducting pilot data recordings, and Malte Naujokat, Jaro Janauschek, and Alexine Leroy for performing the data acquisition. This research was supported by a DFG grant (HE 7520/1-1) to SKH.

Supplementary data

Supplementary data to this article can be found online at https://doi.org/10.1016/j.cortex.2022.02.001.

REFERENCES

Arnal, L. H., Doelling, K. B., & Poeppel, D. (2015). Delta–beta coupled oscillations underlie temporal prediction accuracy. *Cerebral Cortex, 25*(9), 3077–3085.

Arnal, L. H., & Giraud, A.-L. (2012). Cortical oscillations and sensory predictions. *Trends in Cognitive Sciences, 16*(7), 390–398.

Barczak, A., O'Connell, M. N., McGinnis, T., Ross, D., Mowery, T., Falchier, A., & Lakatos, P. (2018). Top-down, contextual entrainment of neuronal oscillations in the auditory thalamocortical circuit. *Proceedings of the National Academy of Sciences, 115*(32), E7605–E7614.

Bates, D., Mächler, M., Bolker, B., & Walker, S. (2015). Fitting linear mixed-effects models using lme4. *Journal of Statistical Software, 67*(1), 1–48.

Bauer, A.-K. R., Jaeger, M., Thorne, J. D., Bendixen, A., & Debener, S. (2015). The auditory dynamic attending theory revisited: A closer look at the pitch comparison task. *Brain Research, 1626*, 198–210.

Berens, P. (2009). CircStat: A MATLAB toolbox for circular statistics. *J Stat Softw, 31*(10), 1–21.

Besle, J., Schevon, C. A., Mehta, A. D., Lakatos, P., Goodman, R. R., McKhann, G. M., Emerson, R. G., & Schroeder, C. E. (2011). Tuning of the human neocortex to the temporal dynamics of attended events. *The Journal of Neuroscience, 31*(9), 3176–3185.

Bouwer, F. L., Fahrenfort, J. J., Millard, S. K., & Slagter, H. A. (2020). A silent disco: Persistent entrainment of low-frequency neural oscillations underlies beat-based, but not memory-based temporal expectations. *bioRxiv*. https://doi.org/10.1101/2020.01.08.899278

Brainard, D. H. (1997). The psychophysics toolbox. *Spatial Vision, 10*(4), 433–436.

Breska, A., & Deouell, L. Y. (2017). Neural mechanisms of rhythm-based temporal prediction: Delta phase-locking reflects temporal predictability but not rhythmic entrainment. *PLoS biology, 15*(2), Article e2001665.

van den Brink, R. L., Wynn, S. C., & Nieuwenhuis, S. (2014). Post-error slowing as a consequence of disturbed low-frequency oscillatory phase entrainment. *Journal of Neuroscience, 34*(33), 11096–11105.

Brunia, C. H. (2003). Cnv and spn: Indices of anticipatory behavior. In *The Bereitschaftspotential* (pp. 207–227). Springer.

Bruns, A. (2004). Fourier-, hilbert-and wavelet-based signal analysis: Are they really different approaches? *Journal of neuroscience methods, 137*(2), 321–332.

Buzsáki, G., & Draguhn, A. (2004). Neuronal oscillations in cortical networks. *Science, 304*(5679), 1926–1929.

Cannon, J. (2021). Expectancy-based rhythmic entrainment as continuous bayesian inference. *PLOS Computational Biology, 17*(6), Article e1009025.

Chang, A., Bosnyak, D. J., & Trainor, L. J. (2019). Rhythmicity facilitates pitch discrimination: Differential roles of low and high frequency neural oscillations. *NeuroImage, 198*, 31–43.

Chaumon, M., Bishop, D. V., & Busch, N. A. (2015). A practical guide to the selection of independent components of the electroencephalogram for artifact correction. *Journal of neuroscience methods, 250*, 47–63.

Chou, E. P., & Hsu, S.-M. (2018). Cosine similarity as a sample size-free measure to quantify phase clustering within a single neurophysiological signal. *Journal of neuroscience methods, 295*, 111–120.

Cohen, M. X. (2014). *Analyzing neural time series data: Theory and practice*. MIT press.

Coull, J. T., Davranche, K., Nazarian, B., & Vidal, F. (2013). Functional anatomy of timing differs for production versus prediction of time intervals. *Neuropsychologia, 51*(2), 309–319.

Cravo, A. M., Rohenkohl, G., Wyart, V., & Nobre, A. C. (2011). Endogenous modulation of low frequency oscillations by temporal expectations. *Journal of Neurophysiology, 106*(6), 2964–2972.

Cravo, A. M., Rohenkohl, G., Wyart, V., & Nobre, A. C. (2013). Temporal expectation enhances contrast sensitivity by phase

entrainment of low-frequency oscillations in visual cortex. *The Journal of Neuroscience, 33*(9), 4002–4010.
Daume, J., Wang, P., Maye, A., Zhang, D., & Engel, A. K. (2021). Non-rhythmic temporal prediction involves phase resets of low-frequency delta oscillations. *Neuroimage, 224*, 117376.
Dercksen, T. T., Widmann, A., Schröger, E., & Wetzel, N. (2020). Omission related brain responses reflect specific and unspecific action-effect couplings. *Neuroimage, 215*, 116840.
van Diepen, R. M., & Mazaheri, A. (2018). The caveats of observing inter-trial phase-coherence in cognitive neuroscience. *Scientific reports, 8*(1), 1–9.
Ding, N., Patel, A. D., Chen, L., Butler, H., Luo, C., & Poeppel, D. (2017). Temporal modulations in speech and music. *Neuroscience and Biobehavioral Reviews, 81*, 181–187.
Doelling, K. B., & Assaneo, M. F. (2021). Neural oscillations are a start toward understanding brain activity rather than the end. *Plos Biology, 19*(5), Article e3001234.
Edwards, E., Soltani, M., Kim, W., Dalal, S. S., Nagarajan, S. S., Berger, M. S., & Knight, R. T. (2009). Comparison of time–frequency responses and the event-related potential to auditory speech stimuli in human cortex. *Journal of neurophysiology, 102*(1), 377–386.
Fisher, N. I. (1995). *Statistical analysis of circular data*. Cambridge University Press.
Giraud, A.-L., & Poeppel, D. (2012). Cortical oscillations and speech processing: Emerging computational principles and operations. *Nature Neuroscience, 15*(4), 511–517.
Gross, J., Kujala, J., Hämäläinen, M., Timmermann, L., Schnitzler, A., & Salmelin, R. (2001). Dynamic imaging of coherent sources: Studying neural interactions in the human brain. *Proceedings of the National Academy of Sciences, 98*(2), 694–699.
Halgren, M., Fabó, D., Ulbert, I., Madsen, J. R., Erőss, L., Doyle, W. K., Devinsky, O., Schomer, D., Cash, S. S., & Halgren, E. (2018). Superficial slow rhythms integrate cortical processing in humans. *Scientific reports, 8*(1), 1–12.
Helfrich, R. F., Fiebelkorn, I. C., Szczepanski, S. M., Lin, J. J., Parvizi, J., Knight, R. T., & Kastner, S. (2018). Neural mechanisms of sustained attention are rhythmic. *Neuron, 99*(4), 854–865.
Henry, M. J., Herrmann, B., & Obleser, J. (2014). Entrained neural oscillations in multiple frequency bands comodulate behavior. *Proceedings of the National Academy of Sciences, 111*(41), 14935–14940.
Henry, M. J., Herrmann, B., & Obleser, J. (2016). Neural microstates govern perception of auditory input without rhythmic structure. *Journal of Neuroscience, 36*(3), 860–871.
Henry, M. J., & Obleser, J. (2012). Frequency modulation entrains slow neural oscillations and optimizes human listening behavior. *Proceedings of the National Academy of Sciences, 109*(49), 20095–20100.
Herbst, S. K., Fiedler, L., & Obleser, J. (2018). Tracking temporal hazard in the human electroencephalogram using a forward encoding model. *eneuro, 5*(2). ENEURO.0017–18.2018.
Herbst, S. K., & Obleser, J. (2017). Implicit variations of temporal predictability: Shaping the neural oscillatory and behavioural response. *Neuropsychologia, 101*, 141–152.
Herbst, S. K., & Obleser, J. (2018). Implicit temporal predictability biases slow oscillatory phase in auditory cortex and enhances pitch discrimination sensitivity. *bioRxiv*, 410274.
Herbst, S. K., & Obleser, J. (2019). Implicit temporal predictability enhances pitch discrimination sensitivity and biases the phase of delta oscillations in auditory cortex. *Neuroimage, 203*, 116198.
Herrmann, B., & Henry, M. J. (2014). Low-frequency neural oscillations support dynamic attending in temporal context. *Timing & Time Perception, 2*(1), 62–86.
Herrmann, B., Henry, M. J., Haegens, S., & Obleser, J. (2016). Temporal expectations and neural amplitude fluctuations in auditory cortex interactively influence perception. *Neuroimage, 124*(Part A), 487–497.
Hincapié, A.-S., Kujala, J., Mattout, J., Pascarella, A., Daligault, S., Delpuech, C., Mery, D., Cosmelli, D., & Jerbi, K. (2017). The impact of meg source reconstruction method on source-space connectivity estimation: A comparison between minimum-norm solution and beamforming. *Neuroimage, 156*, 29–42.
Jones, M. R. (1976). Time, our lost dimension: Toward a new theory of perception, attention, and memory. *Psychological Review, 83*(5), 323–355.
Jones, M. R. (2018). *Time will tell: A theory of dynamic attending*. Oxford University Press.
Jones, M. R., & Boltz, M. (1989). Dynamic attending and responses to time. *Psychological review, 96*(3), 459.
Jones, M. R., Moynihan, H., MacKenzie, N., & Puente, J. (2002). Temporal aspects of stimulus-driven attending in dynamic arrays. *Psychological Science, 13*(4), 313–319.
Keil, J., Pomper, U., & Senkowski, D. (2016). Distinct patterns of local oscillatory activity and functional connectivity underlie intersensory attention and temporal prediction. *Cortex; a Journal Devoted to the Study of the Nervous System and Behavior, 74*, 277–288.
Kösem, A., Gramfort, A., & van Wassenhove, V. (2014). Encoding of event timing in the phase of neural oscillations. *Neuroimage, 92*, 274–284.
Kuznetsova, A., Brockhoff, P. B., & Christensen, R. H. B. (2016). lmerTest: Tests in linear mixed effects models. *R package version 2*, 30.
Lachaux, J.-P., Rodriguez, E., Martinerie, J., & Varela, F. J. (1999). Measuring phase synchrony in brain signals. *Human brain mapping, 8*(4), 194–208.
Lakatos, P., Gross, J., & Thut, G. (2019). A new unifying account of the roles of neuronal entrainment. *Current Biology, 29*(18), R890–R905.
Lakatos, P., Karmos, G., Mehta, A. D., Ulbert, I., & Schroeder, C. E. (2008). Entrainment of neuronal oscillations as a mechanism of attentional selection. *Science, 320*(5872), 110–113.
Lakatos, P., Musacchia, G., O'Connel, M. N., Falchier, A. Y., Javitt, D. C., & Schroeder, C. E. (2013). The spectrotemporal filter mechanism of auditory selective attention. *Neuron, 77*(4), 750–761.
Lakatos, P., Shah, A. S., Knuth, K. H., Ulbert, I., Karmos, G., & Schroeder, C. E. (2005). An oscillatory hierarchy controlling neuronal excitability and stimulus processing in the auditory cortex. *Journal of neurophysiology, 94*(3), 1904–1911.
Lange, K. (2013). The ups and downs of temporal orienting: A review of auditory temporal orienting studies and a model associating the heterogeneous findings on the auditory N1 with opposite effects of attention and prediction. *Frontiers in Human Neuroscience, 7*, 263.
Large, E. W., & Jones, M. R. (1999). The dynamics of attending: How people track time-varying events. *Psychological Review, 106*(1), 119–159.
Lawrance, E. L. A., Harper, N. S., Cooke, J. E., & Schnupp, J. W. H. (2014). Temporal predictability enhances auditory detection. *The Journal of the Acoustical Society of America, 135*(6), EL357–EL363.
Makeig, S., Westerfield, M., Jung, T.-P., Enghoff, S., Townsend, J., Courchesne, E., & Sejnowski, T. J. (2002). Dynamic brain sources of visual evoked responses. *Science, 295*(5555), 690–694.
Maris, E., & Oostenveld, R. (2007). Nonparametric statistical testing of EEG-and MEG-data. *Journal of neuroscience methods, 164*(1), 177–190.
MATLAB. (2019). *Version R2019a*. Natick, Massachusetts: The MathWorks Inc.
Mento, G. (2013). The passive CNV: Carving out the contribution of task-related processes to expectancy. *Frontiers in Human Neuroscience, 7*.

Morey, R. D., & Rouder, J. N. (2018). BayesFactor: Computation of Bayes factors for common designs. *R package version 0, 9*, 12–14.2.
Morillon, B., Arnal, L. H., Schroeder, C. E., & Keitel, A. (2019). Prominence of delta oscillatory rhythms in the motor cortex and their relevance for auditory and speech perception. *Neuroscience and Biobehavioral Reviews, 107*, 136–142.
Morillon, B., & Baillet, S. (2017). Motor origin of temporal predictions in auditory attention. *Proceedings of the National Academy of Sciences, 114*(42), E8913–E8921.
Morillon, B., Schroeder, C. E., Wyart, V., & Arnal, L. H. (2016). Temporal prediction in lieu of periodic stimulation. *The Journal of Neuroscience: the Official Journal of the Society for Neuroscience, 36*(8), 2342–2347.
Neymotin, S. A., Tal, I., Barczak, A., O'Connell, M. N., McGinnis, T., Markowitz, N., Espinal, E., Griffith, E., Anwar, H., Dura-Bernal, S., et al. (2021). Taxonomy of neural oscillation events in primate auditory cortex. *bioRxiv*, 2020–2104.
Niemi, P., & Näätänen, R. (1981). Foreperiod and simple reaction time. *Psychological Bulletin, 89*(1), 133–162.
Nozaradan, S., Peretz, I., Missal, M., & Mouraux, A. (2011). Tagging the neuronal entrainment to beat and meter. *Journal of Neuroscience, 31*(28), 10234–10240.
Obleser, J., Henry, M. J., & Lakatos, P. (2017). What do we talk about when we talk about rhythm? *PLOS Biology, 15*(9), Article e2002794.
Obleser, J., & Kayser, C. (2019). Neural entrainment and attentional selection in the listening brain. *Trends in Cognitive Sciences, 23*(11), 913–926.
Oostenveld, R., Fries, P., Maris, E., & Schoffelen, J.-M. (2011). *Fieldtrip: Open source software for advanced analysis of meg, eeg, and invasive electrophysiological data. 2011*. Computational intelligence and neuroscience.
Oostenveld, R., Stegeman, D. F., Praamstra, P., & van Oosterom, A. (2003). Brain symmetry and topographic analysis of lateralized event-related potentials. *Clinical Neurophysiology, 114*(7), 1194–1202.
Pelli, D. G. (1997). The VideoToolbox software for visual psychophysics: Transforming numbers into movies. *Spatial vision, 10*(4), 437–442.
Pernet, C. R., Wilcox, R. R., & Rousselet, G. A. (2013). Robust correlation analyses: False positive and power validation using a new open source matlab toolbox. *Frontiers in psychology, 3*, 606.
Popov, T., Oostenveld, R., & Schoffelen, J. M. (2018). Fieldtrip made easy: An analysis protocol for group analysis of the auditory steady state brain response in time, frequency, and space. *Frontiers in neuroscience, 12*, 711.
Praamstra, P., Kourtis, D., Kwok, H. F., & Oostenveld, R. (2006). Neurophysiology of implicit timing in serial choice reaction-time performance. *The Journal of Neuroscience, 26*(20), 5448–5455.
Rimmele, J., Jolsvai, H., & Sussman, E. (2010). Auditory target detection is affected by implicit temporal and spatial expectations. *Journal of Cognitive Neuroscience, 23*(5), 1136–1147.
Rimmele, J. M., Morillon, B., Poeppel, D., & Arnal, L. H. (2018). *The proactive and flexible sense of timing*.
Rouder, J. N. (2014). Optional stopping: No problem for Bayesians. *Psychonomic Bulletin & Review, 21*(2), 301–308.
Ruchkin, D. S., Sutton, S., Kietzman, M. L., & Silver, K. (1980). Slow wave and p300 in signal detection. *Electroencephalography and Clinical Neurophysiology, 50*(1–2), 35–47.
Saberi, K., & Hickok, G. (2021). Forward entrainment: Evidence, controversies, constraints, and mechanisms. *bioRxiv*. https://doi.org/10.1101/2021.07.06.451373
Saleh, M., Reimer, J., Penn, R., Ojakangas, C. L., & Hatsopoulos, N. G. (2010). Fast and slow oscillations in human primary motor cortex predict oncoming behaviorally relevant cues. *Neuron, 65*(4), 461–471.
SanMiguel, I., Saupe, K., & Schröger, E. (2013). I know what is missing here: Electrophysiological prediction error signals elicited by omissions of predicted" what" but not" when. *Frontiers in human neuroscience, 7*, 407.
Schmidt-Kassow, M., Schubotz, R. I., & Kotz, S. A. (2009). Attention and entrainment: P3b varies as a function of temporal predictability. *Neuroreport, 20*(1), 31–36.
Schroeder, C. E., & Lakatos, P. (2009). Low-frequency neuronal oscillations as instruments of sensory selection. *Trends in Neurosciences, 32*(1), 9–18.
Schröger, E., Marzecová, A., & SanMiguel, I. (2015). Attention and prediction in human audition: A lesson from cognitive psychophysiology. *The European Journal of Neuroscience, 41*(5), 641–664.
Schürmann, M., Başar-Eroglu, C., Kolev, V., & Başar, E. (2001). Delta responses and cognitive processing: Single-trial evaluations of human visual p300. *International Journal of Psychophysiology, 39*(2–3), 229–239.
Stefanics, G., Hangya, B., Hernádi, I., Winkler, I., Lakatos, P., & Ulbert, I. (2010). Phase entrainment of human delta oscillations can mediate the effects of expectation on reaction speed. *The Journal of neuroscience, 30*(41), 13578–13585.
Tallon-Baudry, C., Bertrand, O., Delpuech, C., & Pernier, J. (1996). Stimulus specificity of phase-locked and non-phase-locked 40 hz visual responses in human. *Journal of Neuroscience, 16*(13), 4240–4249.
Tzourio-Mazoyer, N., Landeau, B., Papathanassiou, D., Crivello, F., Etard, O., Delcroix, N., Mazoyer, B., & Joliot, M. (2002). Automated anatomical labeling of activations in SPM using a macroscopic anatomical parcellation of the MNI MRI single-subject brain. *Neuroimage, 15*(1), 273–289.
Walter, W. G., Cooper, R., Aldridge, V. J., McCallum, W. C., & Winter, A. L. (1964). Contingent negative variation : An electric sign of sensori-motor association and expectancy in the human brain. *Nature, 203*, 380–384.
Wen, H., & Liu, Z. (2016). Separating fractal and oscillatory components in the power spectrum of neurophysiological signal. *Brain topography, 29*(1), 13–26.
Widmann, A., Schröger, E., & Maess, B. (2015). Digital filter design for electrophysiological data – a practical approach. *Journal of Neuroscience Methods, 250*, 34–46.
Wilsch, A., Henry, M. J., Herrmann, B., Maess, B., & Obleser, J. (2015). Slow-delta phase concentration marks improved temporal expectations based on the passage of time. *Psychophysiology, 52*(7), 910–918.
Winkler, I., Debener, S., Müller, K.-R., & Tangermann, M. (2015). On the influence of high-pass filtering on ica-based artifact reduction in eeg-erp. In *2015 37th annual international conference of the IEEE engineering in medicine and Biology society (EMBC)* (pp. 4101–4105). IEEE.
Woodrow, H. (1914). The measurement of attention (1914), volume the psychological monographs. *Google-Books-ID: Jr5nRQAACAAJ, 17*(5).
Wright, B. A., & Fitzgerald, M. B. (2004). The time course of attention in a simple auditory detection task. *Perception & Psychophysics, 66*(3), 508–516.
Zalta, A., Petkoski, S., & Morillon, B. (2020). Natural rhythms of periodic temporal attention. *Nature communications, 11*(1), 1–12.
Zoefel, B., & Heil, P. (2013). Detection of near-threshold sounds is independent of eeg phase in common frequency bands. *Frontiers in psychology, 4*, 262.
Zoefel, B., ten Oever, S., & Sack, A. T. (2018). The involvement of endogenous neural oscillations in the processing of rhythmic input: More than a regular repetition of evoked neural responses. *Frontiers in Neuroscience, 12*.